Optimal Tuning of Active Power Gradient Control for Frequency Support in Multi-Energy Systems

Arcadio Perilla
Intelligent Electrical Power Grids
Delft University of Technology
Delft, Netherlands
A.Perilla@tudelft.nl

Digvijay Gusain
Intelligent Electrical Power Grids
Delft University of Technology
Delft, Netherlands
D.Gusain@tudelft.nl

José Rueda Torres
Intelligent Electrical Power Grids
Delft University of Technology
Delft, Netherlands
j.l.ruedatorres@tudelft.nl

Peter Palensky
Intelligent Electrical Power Grids
Delft University of Technology
Delft, Netherlands
P.Palensky@tudelft.nl

Mart van der Meijden
TenneT TSO B.V.
Delft University of Technology
Delft, Netherlands
Mart.vander.Meijden@tennet.eu

Francisco Gonzalez-Longatt
Institutt for elektro, IT og kybernetikk
Universitetet I Sørøst-Norge
Porsgrunn, Norway
fglongatt@fglongatt.org

***Abstract*—Coping with severe active power imbalances constitutes a challenging task in low inertia multi-energy systems. The phase out of the majority of conventional power plants with large size synchronous generators entails that power electronic interfaced devices should take over the primary task of active power balance-frequency control. In view of this, the active power gradient (APG) control of these devices should be carefully designed to ensure effectiveness and to prevent collateral effects on other stability phenomena. This paper presents two novel formulations for the optimal tuning of the parameters of the APG controllers. Both formulations are defined as a constrained single objective optimization problem. The goal is to optimally manage the APG controllers to quickly bound the instantaneous frequency deviations excited by a large active power imbalance. The first formulation concerns with the minimization of the instantaneous variation of the kinetic energy of the synchronous areas of an interconnected system, whereas the second formulation concerns with the minimization of the spatial displacements between the dynamic trajectories of the time frequency responses in different synchronous areas. The formulations are solved by using a new proposed variant of the mean-variance mapping optimization algorithm (MVMO), and their conceptual implications are illustrated based on numerical simulations performed on a small-size multi-energy system.**

***Keywords*—Active Power Gradient, Electrolysers, Frequency Control, Multi-Energy Systems, MVMO algorithm, VSC-HVDC.**

I. Introduction

Conventional electrical power systems worldwide are evolving towards the so-called multi-energy systems, which are characterized by the predominance of power electronic interfaced devices in generation, transmission, distribution, and responsible consumers. Such systems have a mixture of HVAC and HVDC technologies, and, unlike the conventional power systems, they have to cope with reduced inertia, reduced short-circuit capacity, and variable impedances, which entail unprecedented and faster stability phenomena [1]. Ensuring frequency stability in near future is one of the major concerns raised by different transmission system operators worldwide [2]. Improving and exploiting the capabilities of new technologies of voltage source converters (VSC) is receiving greater attention for different applications in renewable power generation (e.g. wind/solar power plants) [3], high voltage direct current systems (VSC-HVDC) [4], and responsive demand (e.g. multi-megawatt scale electrolysers) [5]. The latest VSC technologies facilitate very fast adjustment of the active power. For instance, an active power gradient (APG), also known by the term 'ramp rate' in existing literature, can be around 1000 MW/s as reported in [6]. To date, the use of APG is being extensively investigated for the case of different types and sizes of renewable generation plants [7], [8]. Moreover, the specifications of the APG functionality is being progressively incorporated in different grid code requirements concerning with the integration of VSCs. For example, specifications for APG as part of the enhanced frequency response (EFR) requirements is taken into account in UK [7].

Finding ways to enhance the performance of the primary frequency control in synchronous areas of a multi-energy system, which are decoupled by VSC-HVDC systems, and as affected by the APG functionality of the VSC stations is an emerging research area. A preliminary research work reported by the authors in [8] showed that the very fast adjustment of the power exchange through the VSC of an embedded HVDC link can significantly support the fast active power-frequency control in synchronous areas with asymmetrical inertia levels and different capabilities for primary frequency control. In [8], it was also found out that the effectiveness of using the APG of VSC-HVDC links to support primary frequency control is limited when the synchronous areas have similar low levels of inertia, and it becomes more complicated if the VSC-HVDC links are also transferring a high amount of active power between the areas. A preliminary research by the authors, reported in [9], showed that the effectiveness of using the APG of VSC-HVDC links can be partially improved via the simultaneous determination of the optimal characteristic of the APG and the smallest required deviation of the active power transfer through the HVDC links. The use of the APG functionality for primary frequency control in large size controllable loads is also an emerging topic. In [10], the feasibility of using APG in multi-megawatt scale Proton Exchange Membrane (PEM) electrolysers was investigated via hardware-in-the loop tests. The results shown in [10], show the feasibility of having prominent APG characteristics in PEM electrolysers.

Going beyond existing literature, this paper takes into account a more complex situation, in which the task of fast active power-frequency control in different synchronous areas is simultaneously taken by the VSC stations of the VSC-HVDC interconnectors and controllable (multi-megawatt scale) PEM electrolysers. The first contribution of the paper concerns with the formulation of two different methods for simultaneous optimal tuning of the APG functionalities and active power deviations of the VSCs units (operating in the VSC-HVDC and the electrolysers).

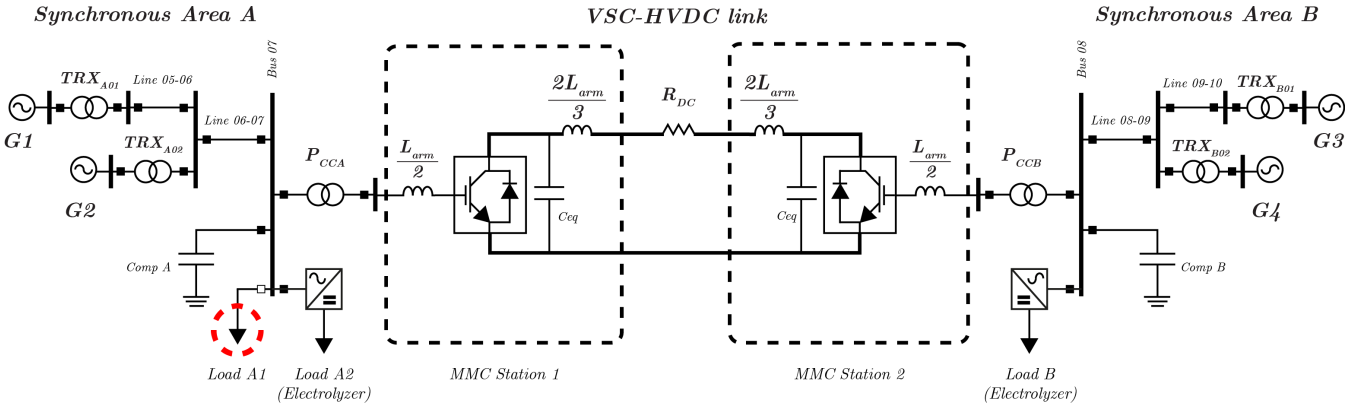

Figure 1. Small-size multi-energy tests system based on the model presented in [9].

The proposed formulations cover the research gap concerning with the lack of insight on the implications of deciding how to tackle the frequency excursions occurring within a synchronous area of a multi-energy system. This problem can be defined from different perspectives depending on what resources are taken into account and how their optimal tuning is formulated. Therefore, the first formulation targets the minimization of the instantaneous variation of the kinetic energy of the synchronous areas, whereas the second formulation targets the minimization of the spatial displacements between the dynamic trajectories of the time frequency responses in different synchronous areas. The numerical simulations of this study are done by using a small-size test multi-energy system (i.e. the focus is on understanding the impact on the dynamic frequency performance), and consider the fact that fast active power-frequency support can be facilitated or not by the VSC-HVDC link that decouples the two synchronous areas of the test system. The paper also contributes with a new proposed variant of the mean-variance mapping optimization algorithm (MVMO), which is used to solve the two proposed formulations of optimization problems within a very reduced computing budget and without modelling simplifications.

The storyline of the next sections of the paper is as follows: Section II presents the rationale and format of the two proposed optimization problems. Section III presents the new variant of the mean-variance mapping optimization (MVMO) algorithm and its application to the proposed problems. Numerical results and the corresponding analysis is provided in Section IV, whereas Section V summarizes the main concluding remarks and also provides an outline for future work.

II. Optimal Tuning of APG

The small test system used in this study is a modified version of the two-area four-machine test system with a HVAC-HVDC transmission network presented in [8]. As illustrated in the single-line diagram shown in Figure 1, the system has two controllable PEM electrolysers that have been added to provide fast active power-frequency support together with the VSC-HVDC interconnector that links the two synchronous areas of the test system. Since the purpose of the research is to investigate the best way to optimize the performance of the APG functionality of the PEM electrolysers and the VSC stations, the option of optimizing or retuning the governors of the synchronous generators of the systems is not considered in this study. Table I summarizes the considered operating condition and also shows that it is assumed that both synchronous areas have a similar level of inertia. Note that the area inertia is relatively low (approx. 13 s) when compared to the inertia of a real synchronous area with a larger number of synchronous generators. In line with the studies reported in [8] and [9], it is considered that an active power imbalance is caused by the sudden decrease of the active power demand in the synchronous area A (cf. red circle shown in Figure 1 that points out the location of the event). This is done via RMS numerical simulations by applying a stepwise decrease of 20% w.r.t. the pre-disturbance active power demand in area A.

The VSC units of the system are represented based on the model presented in [11], which is suitable for RMS simulations of modular multi-level converter (MMC) technology of VSC. Figures 2 and 3 show the APG functionalities defined in this paper, which are used in the model shown in Figure 1 to perform frequency support by the APG functionality for the VSC stations of VSC-HVDC interconnector and the PEM electrolysers, respectively. The characteristics of the APG functionalities will be tuned in a different way when considering the optimization problem formulations presented in the following subsections.

TABLE I. Assumed Operational Scneario and Inertias [8]

Item	Component	Active power (MW)	Inertia Constant H (s)
Generation on Area A	G1	700	6,5
	G2	700	6,5
Demand on Area A	Load A1	250	N/A
	Load A2 (PEM electrolyser)	717	N/A
	MMC station 1	400.5	N/A
Generation on Area B	G3	719	6,175
	G4	700	6,175
	MMC station 2	381.6	N/A
Demand on Area B	Load B (PEM electrolyser)	1767	N/A

A. Problem formulation 1

When an active power imbalance occurs, the dynamic behaviour of the synchronous generators being in operation is excited (instantaneous change of the kinetic energy) and leads to a variation of the electrical frequency within the synchronous area to which the generators belong. This change is also reflected in the measured frequency at the AC side of the VSC stations of HVDC interconnector (e.g. AC buses of the VSC-HVDC link shown in Figure 1). Thus, proper tuning of the APG and the active power deviation (ΔP) from the active power transfer scheduled for the VSC- HVDC interconnector can be considered as feasible means to mitigate

the frequency excursions caused by an active power imbalance. In view of this, and in order to achieve fast control actions with the minimum variation of the total kinetic energy, the first problem formulation has the following format:

Minimize

$$CFA\left(\mathbf{x}^{\mathrm{CFA}}\right)=\int_0^{\tau}\left[\begin{array}{l}\mathrm{w}_1\left(y_i(\mathbf{x}^{\mathrm{CFA}})-y_{1_{\mathrm{ref}}}\right)^2+\\ \ldots+\mathrm{w}_{\mathrm{n}}\left(y_{\mathrm{n}}(\mathbf{x}^{\mathrm{CFA}})-y_{\mathrm{n}_{\mathrm{ref}}}\right)^2\end{array}\right]dt \quad (1)$$

subject to

$$\mathbf{x}_{\min}^{\mathrm{CFA}} \le \mathbf{x}^{\mathrm{CFA}} \le \mathbf{x}_{\max}^{\mathrm{CFA}} \quad (2)$$

where w_i is a weight factor (assumed to be 1 in this study due to the fact that all controlled generators of the studied test system have similar parameters and similar dynamic response), y_i constitutes the instantaneous frequency at the AC side of the VSC station with APG functionality activated, and y_{ref} is defined as the nominal frequency value of the synchronous area. The optimization vector $\mathbf{x}^{\mathrm{CFA}}$ is defined in (3), and its elements (i.e. optimization variables) are $\mathrm{APG_{VSC}}$ and $\Delta\mathrm{P_{VSC}}$ (cf. Figure 2).

$$\mathbf{x}^{\mathrm{CFA}}=[\mathrm{APG_{VSC}}, \Delta\mathrm{P_{VSC}}] \quad (3)$$

The bounds of the optimization variables are taken from [9] and are given below:

$$1\frac{\mathrm{MW}}{\mathrm{min}} < \mathrm{APG_{VSC}} < 60\frac{\mathrm{GW}}{\mathrm{min}} \quad (4)$$

$$0 \le \Delta\mathrm{P_{VSC}} \le P_{VSC\_Rated} \quad (5)$$

This formulation is a virtual attempt (like when using HVAC interconnectors) to enable frequency support between two synchronous areas (by minimizing the instantaneous variation of the kinetic energy of the synchronous areas) via the APG functionality of the VSC-HVDC interconnector.

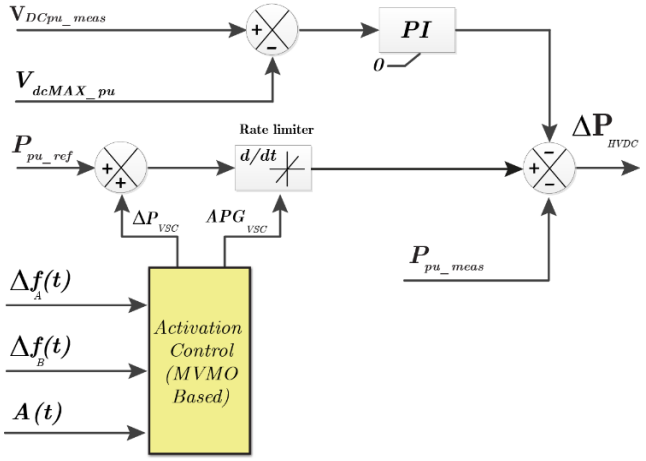

Figure 2. MVMO optimized APG functionality for VSC stations of HVDC interconnectors. Inspired from [9].

B. *Problem formulation 2*

The second problem formulation takes into account the displacements between the dynamic trajectories of the time frequency responses in synchronous areas coupled via VSC-HVDC interconnectors. This is done by considering the product defined in (6), which is a function of the average instantaneous frequency response ω_i in each synchronous area.

$$A(t)=\omega_1(t)\cdot\omega_2(t) \quad (6)$$

In steady-state conditions, A(t) is a constant area. Hence, when an active power imbalance occurs, the derivative of A(t) as defined below by (7) provides an indication of the degree of dynamic frequency excursions in synchronous areas coupled via VSC-HVDC interconnectors (i.e. the optimization problem explicitly takes into account the rate-of-change-of-frequency occurring in each synchronous area).

$$\frac{dA(t)}{dt}=\omega_2\frac{d\omega_1(t)}{dt}+\omega_1\frac{d\omega_2(t)}{dt} \quad (7)$$

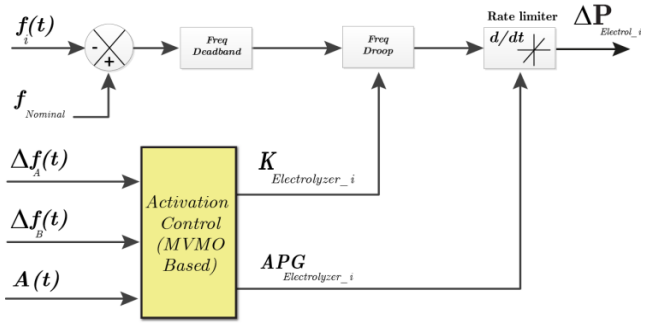

Figure 3. MVMO optimized APG functionality for PEM electrolysers. The deadband is 50 mHz. Inspired from [10].

In view of the rationale explained above, the second problem formulation is proposed according to the following format:

Minimize

$$CFB\left(\mathbf{x}^{\mathrm{CFB}}\right)=\frac{dA(t)}{dt} \quad (8)$$

subject to

$$\frac{d\omega_1(t)}{dt}=\frac{d\omega_2(t)}{dt} \quad (9)$$

$$\mathbf{x}_{\min}^{\mathrm{CFB}} \le \mathbf{x}^{\mathrm{CFB}} \le \mathbf{x}_{\max}^{\mathrm{CFB}} \quad (10)$$

In this formulation, the optimization vector $\mathbf{x}^{\mathrm{CFB}}$ comprises the parameters of VSC shown in Figure 2 ($\mathrm{APG_{VSC}}$ and $\Delta\mathrm{P_{VSC}}$), and the parameters of the PEM electrolysers shown in Figure 3 ($\mathrm{APG_{ELEC\text{-}i}}$ and $\Delta\mathrm{P_{ELEC\text{-}i}}$).

$$\begin{aligned}\mathbf{x}^{\mathrm{CFB}}=[&\mathrm{APG_{VSC}}, \Delta\mathrm{P_{VSC}}, \mathrm{APG_{ELEC\text{-}A}},\ldots\\ &\mathrm{K_{ELEC\text{-}A}}, \mathrm{APG_{ELEC\text{-}B}}, \mathrm{K_{ELEC\text{-}B}}]\end{aligned} \quad (11)$$

The bounds of $\mathrm{APG_{ELEC\text{-}i}}$ and $\Delta\mathrm{P_{ELEC\text{-}i}}$ are taken from [10] and are given below:

$$0\frac{\mathrm{MW}}{\mathrm{s}} < \mathrm{APG_{ELEC\text{-}i}} < 100\frac{\mathrm{MW}}{\mathrm{s}} \quad (12)$$

$$0\frac{\mathrm{MW}}{\mathrm{mHz}} < \mathrm{K_{ELEC\text{-}i}} < 100\frac{\mathrm{MW}}{\mathrm{mHz}} \quad (13)$$

III. Enhanced MVMO Algorithm

The overall procedure of MVMO, as programmed in Python 3.6 is illustrated in Fig. 4. In the initialization stage, random values are drawn for the elements of the optimization

vector. Unlike [12], MVMO is modified in this paper to use latin hypercube sampling (LHS) for instead of random sampling. In this way, it is expected that MVMO covers the whole search space more uniformly and this can lead to a faster convergence. The parameters of MVMO presented in [12] were also used in this paper. RMS simulations are carried out in PowerFactory (version 2019) and the results are exported as csv files. These results are used by the MVMO module to evaluate the objective function value.

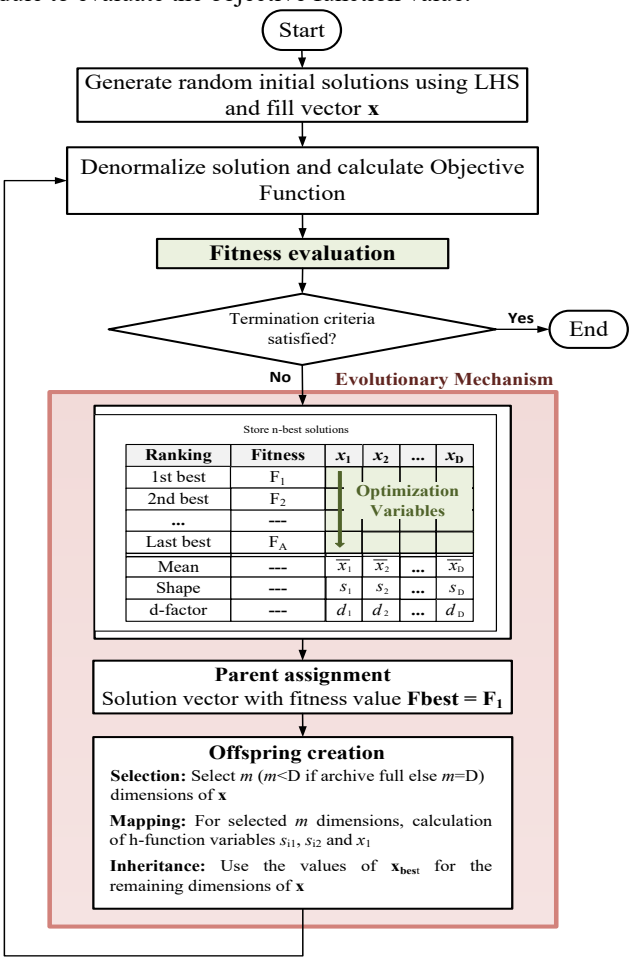

Figure 4. Calculation scheme of the modified MVMO. The fitness evaluation counter is denoted by *i*. Source [12].

MVMO performs the evolution of the solution within a normalized search space, i.e. the values of the elements of the optimization vector are normalized from their [min, max] bounds to the range [0,1]. However, de-normalization of these parameters is performed when the values generated by MVMO are to be used for fitness evaluation. MVMO generates new solutions throughout the optimization process based on the best solution found so far. For this purpose, the algorithm has a solution archive, in which the values of the n-best evolved solutions in the last n-function evaluations are stored. This information is used to compute mean value, variance, and shape factors of each optimization variable. These statistical measures are inputs of the so-called mapping function, which is used to generate a new value of the selected optimization variable from the vector corresponding to the best solution found so far. Details of this function can be found in [12].

The version of MVMO used in this research is enhanced compared to previous versions that helps it to achieve better solutions much faster. It uses a unique mutation strategy, and a proactive scaling factor update method that differentiates it from previous MVMO versions. Within the mutation strategy, it mutates all the elements of the optimization vector of the best fit parent till the solution archive is filled with random solutions to its capacity before switching to user specified number of selected optimization variables. This enables the first population archive to have solutions from all over the search space. The user defined mutations are randomly selected throughout after the initial phase. The statistical metrics, mean and variance, during this initial phase are kept constant at 0.5 to enable wider search for initial good solutions. Afterwards, since the number of mutated particles decrease, so does the computational efficiency. An additional modification of MVMO concerns with the adjustment of the scaling factor (enhancement of the global search capability), which initially increases linearly with number of iterations. However, the algorithm is always checking the objective function values, and stagnation of convergence rates. If the convergence does not improve after multiple attempts, to ensure it is not stuck in a local minima, the scaling factor is updated to a low value (in this version this is set to 2), to enable further exploration of search space. This is done repeatedly whenever no improvements in search space is noticed to ensure the final obtained solution is the global minima. In this paper, there are two termination criterion. One is defined as the fulfilment of a pre-defined number of function evaluations (200), while the other is termination of search if the variance of last 10 solutions being lower than a pre-defined number (1e-4).

IV. Numerical Results

As indicated in Section II, a step decreases of 20% of the active power demand in the synchronous area A is applied in the system at t = 1 s. The time responses of the rotor angle speeds of the four synchronous generators of the system are depicted in Figure 5, considering the optimal tuning of the APG functionalities according to the problem formulation 1, i.e. minimization of $CFA\left(\mathbf{x}^{\mathrm{CFA}}\right)$, or the problem formulation 2, i.e. minimization of $CFB\left(\mathbf{x}^{\mathrm{CFB}}\right)$. Note that each plot of Figure 5 indicates the elements of the optimization vectors considered in each type of objective function, cf. (3) and (11), respectively. The upper left plot of Figure 5 shows the generators' rotor speeds responses obtained when the VSC-HVDC is optimized to provide frequency support to mitigate the active power imbalance occurring in the synchronous area A. Note that the MVMO based optimization (i.e. the best settings are APG_{VSC} = 477 MW/s and ΔP_{VSC} = 134.15 MW) entails a smaller maximum frequency Zenith as well as a faster stabilization of the frequency in a new steady state value closer to the pre-disturbance value, when compared to the case of resorting to the extreme case (i.e. like in emergency conditions) APG_{VSC} = 60 GW/min (or 1 GW/s) and ΔP_{VSC} = 250 MW as indicated defined in [9].

The upper right plot of Figure 5 shows that the optimal tuning according to the problem formulation 2 entails similar dynamic rotor angle responses like in the case of problem formulation 1 (cf. upper left plot), when only the APG_{VSC} and ΔP_{VSC} are adjusted (i.e. the best settings are APG_{VSC} = 961.53 MW/s and ΔP_{VSC} = 114.95 MW) for the VSC-HVDC system.

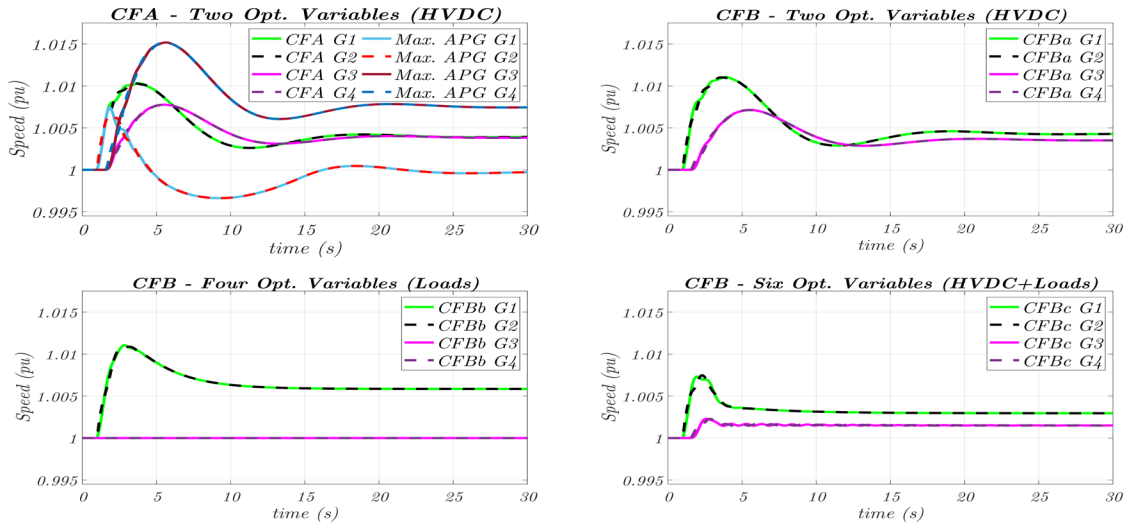

Figure 5. Rotor speed response of the synchronous generators due to a sudden decrease of the active power demand in area A.

The lower left plot of Figure 5 concerns with the case when only $APG_{ELEC\text{-}i}$ and $\Delta P_{ELEC\text{-}i}$ are optimized (i.e. no frequency support by VSC-HVDC system is provided). In this case, the faster response of the PEM electrolyser ($APG_{ELEC\text{-}A}$=97.47 MW/s and $\Delta P_{ELEC\text{-}A}$=14.91 MW/mHz) of area A bounds the frequency deviation in a shorter time period w.r.t. the previous two cases. Finally, the lower right plot of Figure 5 illustrates that a significantly better performance is achieved by using the second problem formulation to simultaneously tune the VSC-HVDC and the PEM electrolysers in both areas (i.e. the best settings are APG_{VSC} = 964.45 MW/s, ΔP_{VSC} = 119 MW, $APG_{ELEC\text{-}A}$=96.46 MW/s, $\Delta P_{ELEC\text{-}A}$=12.37 MW/mHz, $APG_{ELEC\text{-}B}$=96.49 MW/s, $\Delta P_{ELEC\text{-}B}$=96.26 MW/mHz).

V. Conclusions

This paper has two contributions: the proposition of two different formulations for the simultaneous optimal tuning of the APG functionalities and minimization of the active power deviations of the VSCs units (operating in the VSC-HVDC and the electrolysers), as well as an enhanced variant of the MVMO algorithm to quickly find the best settings of the APG functionalities. The numerical results, obtained by using a small size multi-energy system, suggest that the minimization of the instantaneous variation of the kinetic energy of the synchronous areas can be considered as an effective option to quickly bound the maximum frequency deviations caused by active power imbalances. Nevertheless, it was found out that the simultaneous and coordinated minimization of the instantaneous displacements between the dynamic trajectories of the time frequency responses in synchronous areas (coupled via VSC-HVDC interconnectors) entails the most effective mitigation mechanism. So, the second proposed formulation entails the smallest frequency Zenith/Nadir within 2 s after the occurrence of an active power imbalance. The second formulation also entails reaching very quickly a post-disturbance steady-state frequency that is very close to the pre-disturbance steady-state frequency value, while minimizing the deviations of the scheduled active power for both the VSC-HVDC interconnector and the PEM electrolysers. New research effort is being devoted to the analysis of these problem formulations and new formulations in different types of multi-energy systems with several synchronous areas coupled by VSC-HVDC interconnectors.

References

[1] N. A. Masood, R. Yan, and T. Kumar Saha, "Cascading Contingencies in a Renewable Dominated Power System: Risk of Blackouts and Its Mitigation," 2018 IEEE Power & Energy Society General Meeting (PESGM), Portland, OR, 2018, pp. 1-5.

[2] V.N. Sewdien, R. Chatterjee, M. Val Escudero, and J. Van Putten, "System Operational Challenges from the Energy Transition," CIGRE Science & Engineering, vol.17, pp. 5-19, Feb. 2020.

[3] Crăciun, B., Kerekes T., Séra D., Teodorescu R., and Annakkage U., Power ramp limitation capabilities of large PV power plants with active power reserves. *IEEE Transactions on Sustainable Energy*, vol. 8, no. 2, pp. 573–581, 2017.

[4] Karaolanis, A., Perilla A., Rueda, J.L., van der Meijden M., and Alefragkis A., Generic model of a VSC-based HVDC link for RMS simulations in PSS/E. IFAC-PapersOnLine, vol. 51, no. 28, pp. 303 – 308, *10th IFAC Symposium on Control of Power and Energy Systems* CPES, 2018.

[5] F. Alshehri. V. García Suárez, J.L. Rueda Torres, A. Perilla, and M.A.M.M van der Meijden, "Modelling and evaluation of PEM hydrogen technologies for frequency ancillary services in future multi-energy sustainable power systems," Heliyon, vol. 5, no. 4, pp. 1-24, April 2019..

[6] Wang, W., Beddard, A., Barnes M., and Marjanovic O., Analysis of active power control for VSC HVDC, *IEEE Transactions on Power Delivery*, vol. 29, no. 4, pp. 1978–1988, 2014.

[7] Sanchez, F., Gonzalez-Longatt F., and Bogdanov D., Probabilistic assessment of enhanced frequency response services using real frequency time series. *20th International Symposium on Electrical Apparatus and Technologies* (SIELA), pp. 1–4, 2018.

[8] S. Rüberg et al, "Deliverable D1.6: Demonstration of Mitigation Measures and Clarification of Unclear Grid Code Requirements," Public report of the MIGRATE H2020 project, Dec. 2019.

[9] A. Perilla, J.L. Rueda Torres, M.A.M.M van der Meijden, E. Rakhshani, Peter Palensky, and A. Alefragkis, "MVMO-based tuning of Active Power Gradient Control of VSC-HVDC links for Frequency Support," 2nd International Conference on Smart Grid and Renewable Energy, Doha, Qatar, Nov. 2019.

[10] J.L. Rueda Torres et al, "TSO2020 Activity 2: Stability Analysis of an International Electricity System connected to Regional and Local Sustainable Gas Systems," Public report of the TSO2020 project. December 2019.

[11] CIGRE Working Group B4-57, Guide for the Development of Models for HVDC Converters in a HVDC Grid," CIGRE, Tech. Rep, 2014.

[12] J.L. Rueda, and I. Erlich, "Hybrid Single Parent-Offspring MVMO for Solving CEC2018 Computationally Expensive Problems," 2018 IEEE World Congress on Computational Intelligence, pp.1-8, Rio de Janeiro, Brazil, July 2018.